

5-2015

Hand Pattern Recognition Using Smart Band

Theerth Raj Munusamy
University of Arkansas, Fayetteville

Follow this and additional works at: <http://scholarworks.uark.edu/etd>

 Part of the [Biomedical Devices and Instrumentation Commons](#), and the [Electronic Devices and Semiconductor Manufacturing Commons](#)

Recommended Citation

Munusamy, Theerth Raj, "Hand Pattern Recognition Using Smart Band" (2015). *Theses and Dissertations*. 1126.
<http://scholarworks.uark.edu/etd/1126>

This Thesis is brought to you for free and open access by ScholarWorks@UARK. It has been accepted for inclusion in Theses and Dissertations by an authorized administrator of ScholarWorks@UARK. For more information, please contact scholar@uark.edu, ccmiddle@uark.edu.

Hand Pattern Recognition Using Smart Band

Hand Pattern Recognition Using Smart Band

A thesis submitted in partial fulfillment
of the requirements for the degree of
Master of Science in Electrical Engineering

By

Theerth Raj Munusamy
Anna University
Bachelor of Engineering in Electronics and Communication, 2011
Saveetha University
Master of Engineering in Robotics, 2013

May 2015
University of Arkansas

This thesis is approved for recommendation to the Graduate Council.

Dr. Vijay K. Varadan

Dr. Juan C Balda

Dr. Roy McCann

ABSTRACT

The Importance of gesture recognition has widely spread around the world. Many research strategies have been proposed to study and recognize gestures, especially facial and hand gestures. Distinguishing and recognizing hand gestures is vital in hotspot fields such as bionic parts, powered exoskeleton, diagnosing muscle disorders, etc. Recognizing such gesture patterns can also create a stress-free and fancy user interface for mobile phones, gaming consoles and other such devices.

The objective is to design a simple yet efficient wearable hand gesture recognizing system. This thesis also shows that by taking both EMG and accelerometer data into account, can improve the system to recognize more patterns with higher accuracy levels. For this, a hand band embedded with a triple axis accelerometer and three surface EMG electrodes is employed to source the system. The non-invasive surface EMG electrodes senses muscle action while the accelerometer senses the hand motions. The EMG signal is passed through analog front-end module for noise filtering and signal amplification. An ARM Cortex processor converts the analog EMG and accelerometer signal into digital and transmits to a PC via Bluetooth protocol. On the receiver section, the raw EMG and acceleration data is further processed and decomposed offline using MATLAB tools to extract features such as root mean square, waveform length, threshold crossing, variance and mean. Extracted features are then fed through multi-class SVM (Support Vector Machine) process for pattern recognition. The chapters below discuss in greater detail on pattern recognition technique and other modules involved.

ACKNOWLEDGEMENT

It is with utmost sincerity that I extend my deep and heartfelt thanks to my thesis advisor Dr. Vijay K. Varadan, who has the attitude and substance of a genius: he continually and convincingly conveyed a spirit of adventure in regard to research and scholarship, and an excitement in regard to teaching. His expertise in wireless health care system improved my research skills and prepared me for the future challenges. I could not have imagined having a better advisor and mentor for my master study.

Besides my advisor, I would like to thank the rest of my thesis committee: Dr. Juan C Balda and Dr. Roy McCann for their encouragement, insightful comments, and hard questions.

To my friends: without your encouragement, help, and support, I do not know how I would have made it through this course of work. More specifically, many thanks to Mouli Ramasamy: you kept me focused, cleared away the doubts that cropped up for me, and were such a tremendous guide throughout this thesis. I am lucky to have a friend like you.

Finally, to my family: my parents have been a big influence in getting me to this point in my life, and it is through their support, their constant care of all of my wishes, aims, and ambitions that have led me to where I am today. I can say with absolute certainty that without you, without the support of my brothers, sisters and uncle, I would not be here. I dedicate this thesis to all of you.

TABLES OF CONTENTS

1. INTRODUCTION	1
1.1. Electromyography	1
1.2. Electrical Characteristics	2
1.3. EMG Electrodes	2
1.4. EMG Signal Decomposition & Processing	4
1.5. Proposed System and Thesis Structure	5
2. STATE OF ART AND LITERATURE	7
2.1. Sources of Noise	7
2.2. Techniques Involved in EMG Signal Processing	8
2.3. Accelerometer Based Pattern Recognition	10
2.4. Vision Based Recognition of Hand Gestures	11
2.5. Thermal Scanning	12
2.6. EMG Based Hand Pattern Recognition	13
3. FILTERS AND AMPLIFIERS	14
3.1. Low Pass and High Pass Filter	14
3.2. Operational Amplifier	15
3.2.1. Non-Inverting Low Pass Amplifier	16
3.2.2. Bessel Filter	17
3.3. Instrumentation Amplifier	19
4. MEMS ACCELEROMETER	21
4.1. Introduction	21
4.2. Technical Specifications	22

5. BLUETOOTH – WIRELESS PROTOCOL	23
5.1. Introduction	23
5.2. Technical Specifications	24
5.3. Advantages of Bluetooth over other Communication Protocols	25
6. SYSTEM DESIGN	26
6.1. Introduction	26
6.2. Hardware Design	27
6.2.1. Sensors	28
6.2.2. Analog Front End	29
6.2.3. Microcontroller	32
6.2.4. Wireless Transmission	34
6.3. Software Design	34
6.3.1. Transmitter Section	34
6.3.2. Receiver Section	37
7. TEST AND RESULTS	43
7.1. Testing Procedure	43
7.2. Results on Pattern Recognition	43
8. CONCLUSION AND FUTURE DEVELOPMENTS	44
REFERENCES	45
APPENDIX	49

LIST OF FIGURES

Figure 1.1 – Block diagram of a simple electromyograph	1
Figure 1.2 – Surface Electrode and Needle Electrode	3
Figure 1.3 – MUAP recorded on same motor unit but at different locations	5
Figure 2.1 – Linear - Support Vector Machine	9
Figure 2.2 – Accelerometer based Hand pattern recognition	10
Figure 2.3 – Vision Based Hand Gesture Recognition	11
Figure 2.4 – Block diagram of hand pattern recognition using thermal image	12
Figure 2.5 – EMG processing using Multilayer Neural Networks	13
Figure 3.1 – Frequency response of Low Pass Filter and High Pass Filter	14
Figure 3.2 – Low Pass Filter and High Pass Filter	15
Figure 3.3 – Non-Inverting Low Pass Filter	16
Figure 3.4 – 3 rd Order Besselworth Filter	17
Figure 3.5 – Frequency response, group delay and step response of Bessel filter	18
Figure 3.6 - Instrumentation Amplifier	19
Figure 4.1 – Axes of acceleration sensitivity	21
Figure 4.2 – ADXL335 Triple Axis Accelerometer	22
Figure 5.1 – Bluetooth HC-05 Module	24
Figure 6.1 – System Design	27
Figure 6.2 – Smart Band	28
Figure 6.3 – Front End Amplifier Design	29
Figure 6.4 – Analog Front End and Bluetooth – Schematic	30
Figure 6.5 – Microcontroller (CPU) – Schematic	33
Figure 6.6 – Transmitter Software Flow	36

Figure 6.7 – Receiver Software Flow	37
Figure 6.8 – Raw EMG signal, Full-length Rectified EMG Signal and FIR filtered EMG signal	39
Figure 6.9 – Raw EMG signal, Accelerometer Reading for X-Axis and Accelerometer Reading for Y-Axis during Wrist Pronation	40
Figure 6.10 – Transmitter Hardware	42

LIST OF TABLES

Table 4.1 – Technical specifications of Accelerometer	22
Table 5.1 – Technical specifications of Bluetooth Technology	25

1. INTRODUCTION

1.1. Electromyography

Electromyography (EMG) is a practice adopted for evaluating and recording the electrical / neural activity of muscle tissue, using small electrodes attached to the skin or inserted into the muscle. It is most commonly represented as a visual display or audible signal. The device which plots this activity is called an electromyograph and the device which records this signal is called an electromyogram. EMG bio-potential signals are very sensitive to the muscle activity. This makes it a great tool for a variety of clinical and bio-medical applications. Clinical applications mainly include: diagnosing abnormalities in the muscular activity, nerve dysfunction or to analyze bio-mechanics of human or animal body movements ^[1].

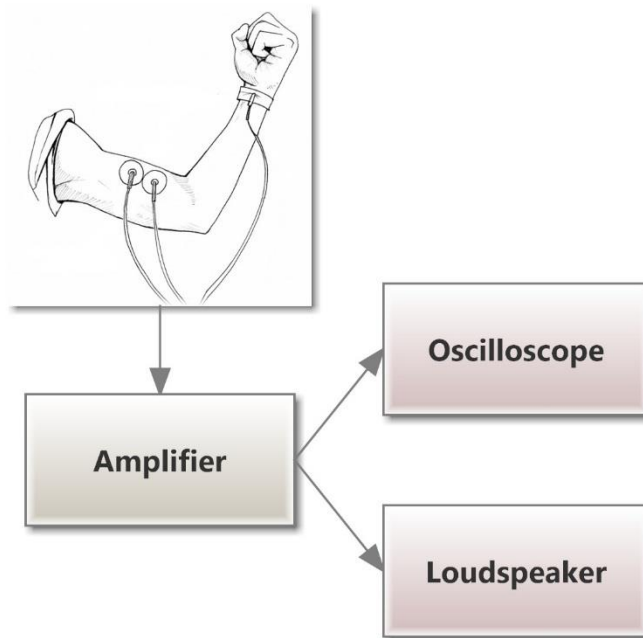


Figure 1.1 – Block diagram of a simple electromyograph

An electrical signal is recorded at both instances: when the muscle is resting and when activated. Featuring parameters such as frequency, voltage and shape are taken into account and examined. Any abnormal readings indicate the presence of some muscle / nerve damage.

A motor unit is defined as the one motor neuron and all of the muscle fibers it innervates. When a motor unit fires, the impulse (called an action potential) is carried down the motor neuron to the muscle. The area where the nerve contacts the muscle is called the neuromuscular junction, or the motor end plate^[2].

1.2. Electrical Characteristics

The measured EMG potentials range between 0-10mV peak-to-peak depending upon the muscle under observation and electrode placement. The frequency range for examining the muscle contraction and relaxation lie 0.5Hz-500Hz^[3]. To be more particular, it is necessary to set the cut-off frequency of a low pass filter to 450Hz.

1.3. EMG Electrodes

The bio-potential electrodes are used to pick up EMG signals. Bio-potential electrodes are designed to operate under low voltage and low current^[4]. Electrodes convert the ionic currents generated by the muscles into electrical signals^[5]. There are two types of EMG electrodes: Intramuscular EMG and Surface EMG electrodes. To perform an

intramuscular EMG, a needle, or a needle containing two fine-wire electrodes, is inserted through the skin into the muscles tissue. Intramuscular EMG provides the state of the muscle and its innervating nerve; this method may be considered too invasive or unnecessary in some cases. Instead, a non-invasive approach, surface EMG electrodes are placed on the skin just above the muscle which needs to be studied. Comparing both, since needle electrode gets a direct contact with the muscle, it is capable of picking up more sensitive and informational data than surface EMG electrodes. The invasive method involves a small risk of bleeding or air leak when a needle is inserted into a muscle.



Figure 1.2 – Surface Electrode (Left) and Needle Electrode (Right)

It is not advisable to use needle electrode on older people who may experience skin damage while installing and removing surface electrode. Skin preparations are not mandatory for recording EMG signals using surface electrodes, but in some cases, due to excess fat or when you need better readings, it is necessary. Preparation of skin mainly involves removing the hair and cleansing the skin with antiseptic lotion.

1.4. EMG Signal Decomposition & Processing

The bio-potential signal recorded is a constituent of various motor unit action potentials (MUAP) from various motor units. Therefore, placement of electrodes tends to play a major role in recording EMG signals. Electrodes placed on different motor unit shows distinct readings. Whereas, electrodes placed on the same motor unit at different locations may have almost the same MUAP readings with slight variations in frequency and amplitude^[6]. It is easy to visually identify the abnormalities in the signals when two or three MUAPs are involved; but it becomes impossible to distinguish when four or more MUAPs are taken into account. This challenge attracts the researchers around the world and many approaches have been documented for decomposing EMG signals. Yet, it is impossible to completely decompose EMG signals into their respective MUAPs to obtain precise readings.

In nature, raw EMG signals represent both negative and positive components along with some noise. Therefore, it is compulsory to process the signal before extracting the information to make the results more precise. The negative and positive components in the raw signal raw EMG signals may average to zero. Rectification is a widely adopted methodology to overcome this problem. There are two types of rectification: Full-length and half-length. Full-length rectifications convert the negative components of the signal into positive components; whereas, half-length rectification remove the negative components of the signal. In other words the difference between the two rectifications is that a full-length rectification takes the absolute value of the entire data^{[7][8]}. Full-length rectification has more advantage than half-length since it preserves the entire set of data which is essential to make the results more accurate.

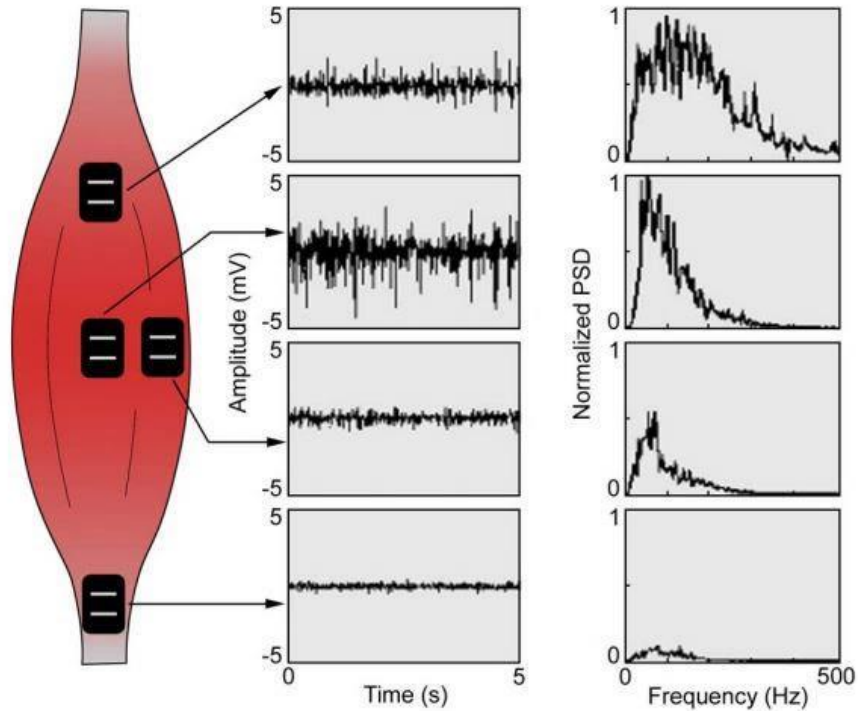


Figure 1.3 – MUAP recorded on same motor unit but at different locations ^[6]

1.5. Proposed System & Thesis Structure

One of the challenging approaches in the wearable technology and human machine interface (HMI) field is to link bio-signals with the device that needs to be controlled. This thesis focuses on designing an efficient wearable gesture recognizing smart band. The smart band is capable of measuring electrical activity in muscle and hand movement instantly. These signals are then interpreted and translated into useful computer commands. Along with the bio-potential signal the smart band is outfitted with an accelerometer sensor which helps to recognize the pattern with much more accuracy. An ARM processor is interfaced with a Bluetooth 4.0 module which helps to collect and transmit the samples to a PC. The receiver

processes these signals through a FIR filter to remove the noise and then pass them for full-length rectification and multi-class SVM for feature extraction and pattern extraction.

This thesis is structured in a way to clearly detail the methods and procedures adopted to fulfill the needs of a proposed system. Chapter 2 describes the design, working and functions of different analog filters, such as high pass and low pass filters, instrumentation amplifier, low pass and band pass amplifier. Chapter 3 gives you an overall idea about Bluetooth technology along with its advantages over other communication protocols. Chapter 4 describes the basics of MEMS technology and also details the specification of the accelerometer sensor used. Chapter 5 briefs the overall system architecture which includes hardware design, software design and pattern recognition technique with various plots and flow charts for better understanding. Chapter 6 details the testing procedures and results attained by this work. Chapter 7 describes the conclusion and the future work that can be incorporated in this thesis.

2. STATE OF ART AND LITERATURE REVIEW

Recognizing hand gesture has a huge potential, especially in the field of human-computer interaction and user-interface applications. The fundamental block of a gesture recognition system includes data acquisition, gesture modeling, feature extraction and hand gesture recognition. Different tools have been proposed for hand gesture recognition, mainly approaches based on computer vision, 3-D modeling, statistical modeling, template matching, neural networks, etc.^[9]. Some of them are discussed below in detail.

2.2.1. Sources of Noise

Amplitude of the EMG signal is random in nature, therefore, the occurrence of noise normal. Understanding the sources and elimination of noise is vital for better results. There are three types of noise: transducer noise, ambient noise and motion artifacts noise.

Transducer noise: As the name indicates, this noise has its origin in the electrode. There are two types of transducer noise: DC voltage potential and AC voltage potential. The DC voltage potential is caused by the difference in the impedance between the skin and the electrode, and the chemical reactions occurring due to the conductive gel. The AC voltage potential is caused by the variation in impedance between the conductive transducer and the skin^[6].

Ambient Noise: This is caused by common factors such as power supply, magnetic radiation, radio waves, force plates, ECG intervention, etc., and has a wide range of

frequency components. An AC power source has more influence when compared to other factors; therefore, the frequency mostly lies in the range of 50-60Hz ^[6].

Motion Artifacts: These caused by two factors: disturbance between the skin and the electrode, and movement of the cable connecting the electrode and analog front end amplifiers. They can be suppressed by proper sensor placement and effective cabling ^[6].

2.2.2. Techniques involved in EMG Signal Processing

EMG signal processing is a fundamental block to eliminate the noises from the raw EMG signal and recognize the pattern. Artificial neural networks, principal component analysis, wavelet analysis and support vector machine are discussed below:

Principal Component Analysis: PCA is used to reduce a large set of data variables using orthogonal transformation; it converts correlated variables with more variability into principal components. PCA mainly helps when only a few variables contain information in a large set of variables ^[10]. Therefore, the number of uncorrelated variables is always less than or equal to the original data set. PCA is normally done by using a square matrix; this becomes complicated when more than two variables exist.

Wavelet Analysis: Wavelet transformation can be used for both continuous and discrete signals; unlike Fourier transformation, wavelet analysis translates a signal into wavelets ^[11]. Wavelet analysis is localized in the frequency and time region of the signal, but the cross-term effect is noisy which makes it unsuitable when more than one component is present ^[12].

Artificial Neural Networks: ANN is capable of predicting a result based on a large set of data with interconnection, which makes ANN best suited to predict neuromuscular diseases or other disorders ^[13]. ANN consists of hidden layers called neurons which connect the input and output layers. These neurons are weighted based on the interconnection and it must be periodically updated for best results. Training of an ANN system consumes more time when compared to other techniques, especially when there are more hidden layers.

Support Vector Machine: SVM is a supervised learning model that is capable of analyzing large data sets to recognize a pattern. SVM can be classified into linear, non-linear and soft margins. Classification is done based upon the training and test sets. Figure 2.1 shows the difference between the three types of SVM. Training and test sets with large margins will be more efficient and accurate. Simple SVM, also called binary SVM can only be used to identify between two classes. If more than two classes can be predicted, multi-class SVM can be used or more layers of binary SVMs can be designed.

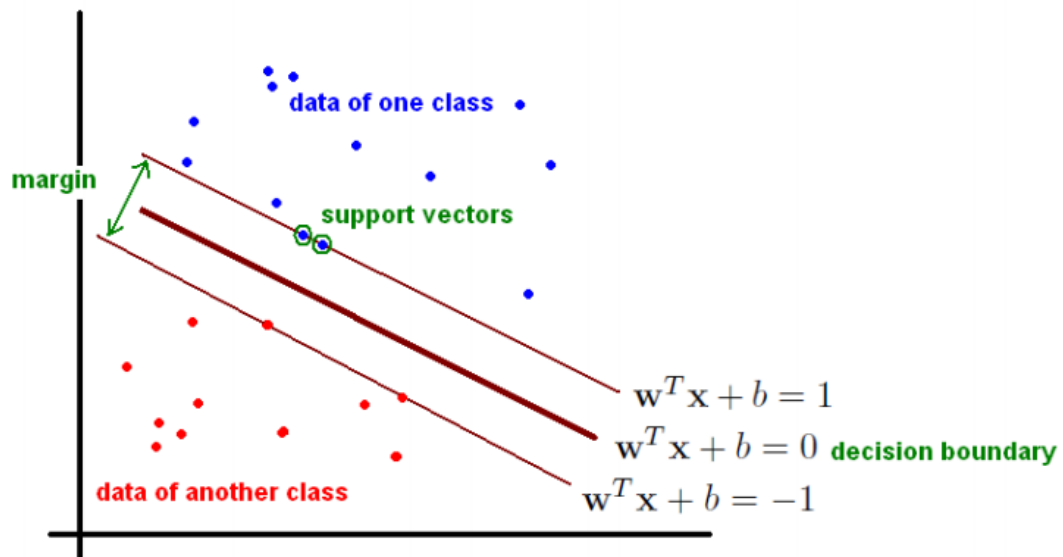


Figure 2.1 – Linear - Support Vector Machines ^[14]

2.2.3. Accelerometer Based Pattern Recognition

An acceleration based gesture recognition system may use one or more 3- axis accelerometer as input source. Like any other pattern recognition system, it initially collects the acceleration data for different hand postures. This data is fed through the signal processing unit for wave shaping and noise reduction. Lastly, the features are extracted and further processed for pattern recognition. Different pattern recognition approaches may be handled, but Frame-based Descriptor and multi-class SVM (FDSVM) are widely used which yield better results ^[15]. A model of accelerometer based pattern recognition is best shown below in the figure 2.2. This methodology is a great fit to recognize the posture or orientation of the hand/palm; to recognize the finger movements a glove inbuilt with separate accelerometers for individual fingers is necessary. This increases the complexity of software and hardware section. And this method is only restricted to identify the gestures based on orientation and movements; it is not possible to identify finger/hand gestures that has no rotation along the axis of accelerometer.



Figure 2.2 – Accelerometer based Hand pattern recognition ^[16]

2.2.4. Vision Based Recognition of Hand Gestures

Unlike the previous method, techniques that require a CCD camera as an input source can be classified as Vision based gesture recognition. It commonly involves software based image processing and template matching technique. In this technique, a video covering the hand pattern is first decomposed into individual frames and selects a frame which has best detail. The selected frame is then fed into the system for further decomposition and processing. Initially the system is programmed and trained with a set of images stored in the database. When a new input image is fed, the system processes the image (i.e. it filters the noise and subtracts the background) and finds the best match with the images stored in the database. Based on the match the system produces an output. Other image processing techniques involve edge detection, principal component analysis, boosting, contour and silhouette matching, model based recognition and Hidden Markov Model (HMM) ^[17]. An example of finger-tip detection is shown below in the figure 2.3. This vision based technique is void when the environment is dark or when the contrast between the skin and background is dull or almost same (i.e. the system becomes inefficient in differentiating skin texture and background). This is because; the system becomes incapable of differentiating and isolating the hand from its background and thus stops further processing.



Figure 2.3 – Vision Based Hand Gesture Recognition ^[17]

2.2.5. Thermal Scanning

Thermal scanning is very similar to that of the vision based hand pattern sensing. The only difference is that the system is trained with a set of thermal images taken with a thermal camera or an infrared camera. These cameras sense the heat radiated body or an object, in this case, the camera senses the heat radiated by the hand. This helps to identify and recognize patterns even when there is dirt, cut or wound on the hand. The main advantage of this technique over vision based sensing is that thermal camera is resistant to noise and independent of light; i.e. thermal camera is capable of taking images in the dark and also eliminates the contrast and brightness error which is present in the vision based hand sensing. Presence of noise is less when compared to the CCD camera technique. The features are extracted from the gray scale of the image. Rest of the processing and pattern recognition is very similar to that of the vision based sensing ^[18]. A block diagram representing gesture recognition system using thermal images is shown below in figure 2.4. The efficiency of this technique degrades as the background temperature and the hand temperature equals.

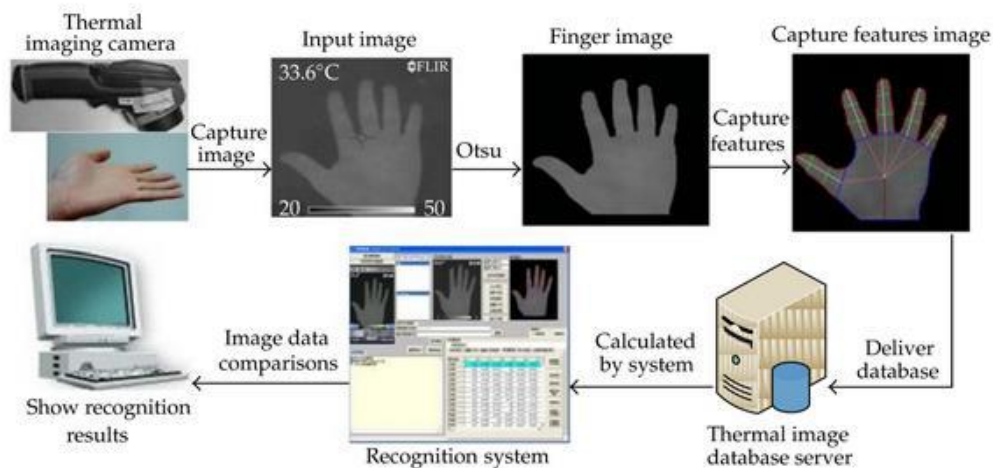


Figure 2.4 – Block diagram of hand pattern recognition using thermal image ^[18]

2.2.6. EMG Based Hand Pattern Recognition

EMG based pattern recognition challenges have been trending in the recent years; especially in the field of prosthetic hand, gaming, control devices, etc. Surface EMG electrodes are commonly used for this application. For better results, three to four channels are used to pick up EMG signals and amplified. Later, the signals are converted to digital format and further processed using digital filters. Wavelet transformation, FIR filter and IIR Filter are the most widely used digital filters. The signal is then decomposed to extract the features representing the hand gestures. Important features carrying the gesture information include root mean square (RMS), standard deviation and mean absolute value (MAV) in time domain. Finally, these features are classified to recognize the pattern. The major drawback of EMG based approaches is that it requires two or more than two channels to increase the accuracy and it does not capture patterns based on hand movements.

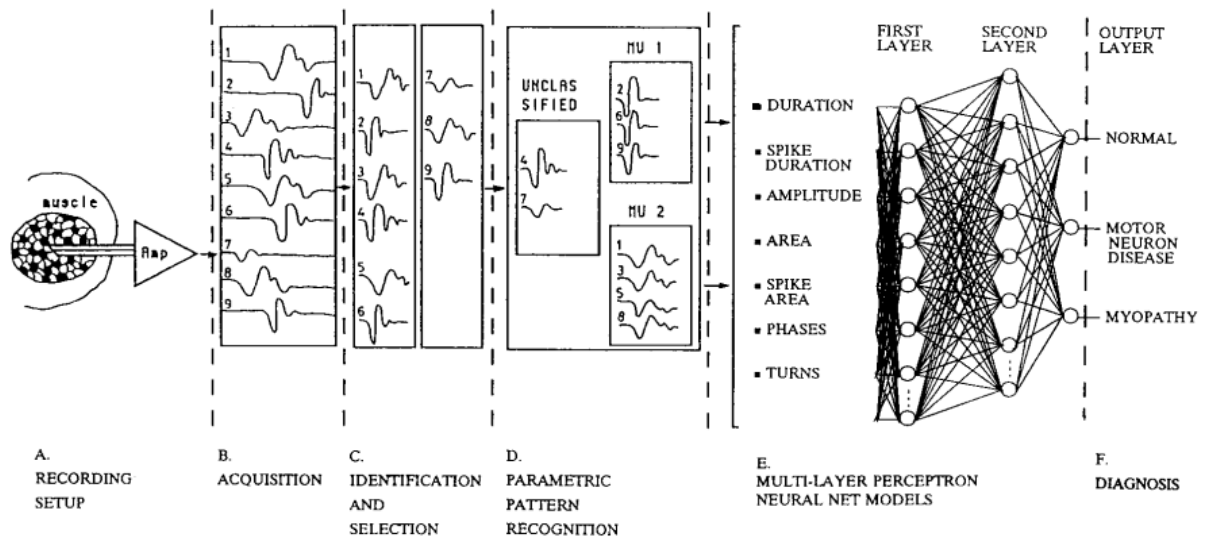


Figure 2.5 – EMG processing using Multilayer Neural Networks ^[19]

3. FILTERS AND AMPLIFIERS

3.1. Low Pass and High Pass Filter

Filters can be classified into active and passive filters. As the name indicates, active filter consists of active components such as op-amps, transistors, etc. while the passive filter includes only resistors, capacitors and other such frequency dependent components. The main disadvantage of the passive filter over the active filters is that the amplitude of the output signal is always less than the input signal. Filters can be classified into High pass and Low pass filter. As the names indicate, high pass filter allows only frequencies above the cut-off frequency (f_c), whereas low pass filter allows frequencies below the cut-off frequency (f_c) of the filter. The frequency response of a High pass and low pass filter is shown below (Figure 3.1).

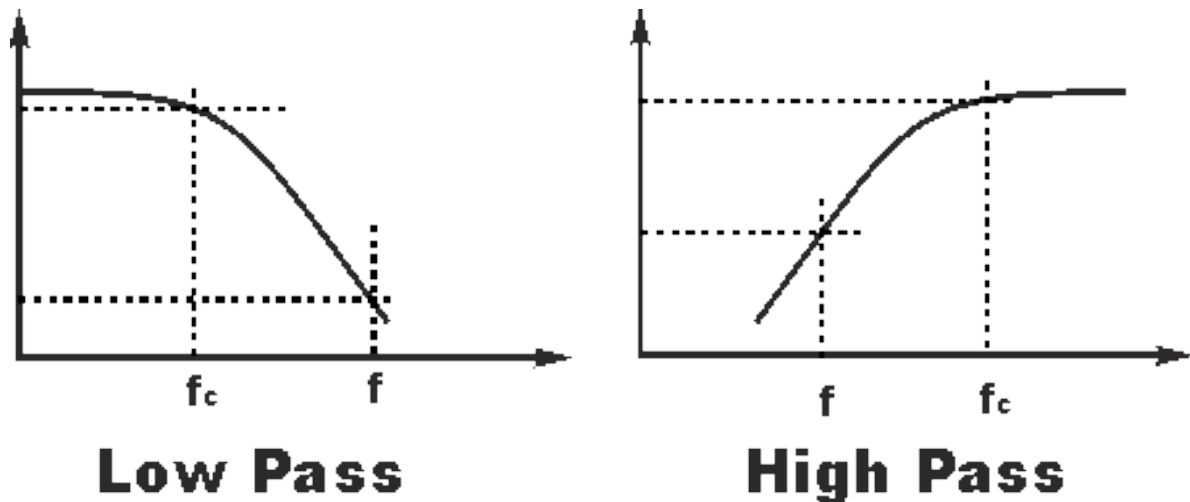


Figure 3.1 – Frequency response of Low Pass Filter and High Pass Filter

A simple first order RC high pass filter is shown below in the figure 3.2. The cut-off frequency is given by the formula:

$$\text{Cut-off frequency, } f_c = \frac{1}{2\pi RC} \text{ Hz}$$

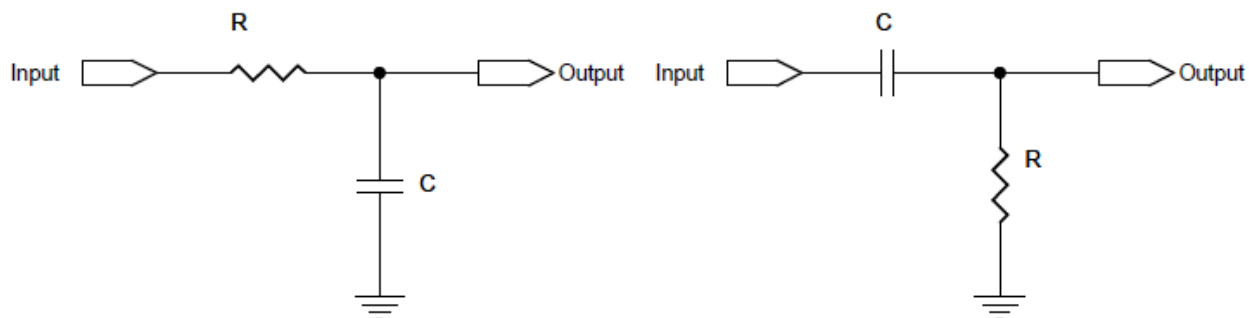


Figure 3.2 – Low Pass Filter (Left) and High Pass Filter (Right)

3.2. Operational Amplifier

An op-amp is an electronic circuit which amplifies the input signal in terms of voltage or current. And also, op-amps can be used condition the signals in terms of frequency, such circuits are called as active filters. An ideal op-amp has these characteristics: infinite voltage gain, infinite bandwidth, infinite input impedance, infinite Common Mode Rejection Ratio (CMRR), zero output impedance, zero input offset voltage and zero noise. Unlike passive filters, the bandwidth and frequency response can be altered effectively in an op-amp circuit. Active filters can be designed for low pass, high pass and bandpass filtering. Such filters are classified by the number of frequency dependent components employed and named as first order, second order, third order and so on. A simple RC filter is recognized as first order since only one capacitor is used.

2.2.1 Non-Inverting Low Pass Amplifier

A low pass amplifier is basically a filter that amplifies low frequency signals and attenuate signals with frequencies above the cut-off frequency (f_c). The feedback loop provides good stability and very high input impedance. The gain of the amplifier depends upon the resistors connected to the inverting terminal of the op-amp. RC combinations connected to the non-inverting terminal of the op-amp decide the cut-off threshold. A simple non-inverting low pass amplifier is shown below (Figure 3.3).

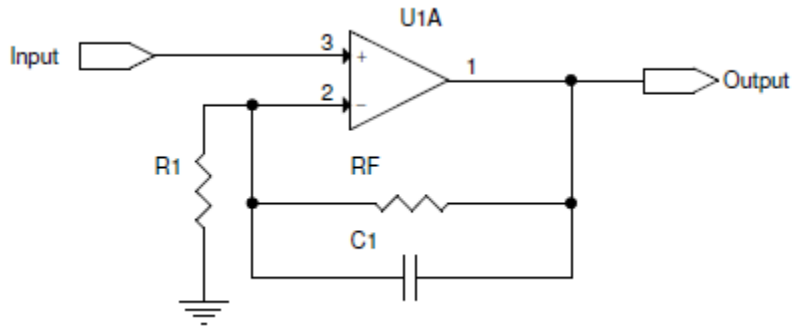


Figure 3.3 – Non-Inverting Low Pass Filter

$$Gain = 1 + \frac{R_F}{R_1}$$

$$Cut - off \ frequency, \quad f_c = \frac{1}{2\pi R_F C_1} \text{ Hz}$$

The gain of the amplifier depends upon the frequency of the output signal. For low frequency signals, the circuit increases the gain of the amplifier and for high frequencies the gain decreases ^[20].

2.2.2 Bessel Filter

Bessel filter is named after a German mathematician Friedrich Bessel, who developed the mathematical model of this filter. It is also called as Bessel Thomson filter, named after W.E. Thomson who applied the mathematical model to design the actual working filter. Bessel filter is very similar to Gaussian filter; but it has better group delay, shaping factor and flat phase delay than the Gaussian filter of the same order. In other words, it has better amplitude and transient behavior when compared to other filters. For a square wave input, the Bessel filter can reproduce the input without any overshoot, but at the cost of slower attenuation rate above the cut-off frequency ^[21]. The frequency response, group delay and step response of Bessel filter is shown below (Figure 3.5).

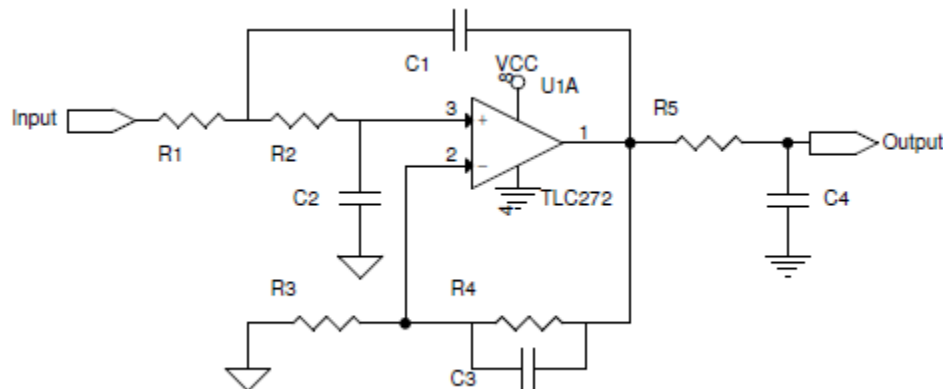


Figure 3.4 – 3rd Order Besselworth Filter

When the frequency of the input signal is less than the cut-off frequency ($f \ll f_c$), impedance of the $R_4 C_3$ connected in parallel is dominated by the resistor R_4 ($R_4 \parallel C_3 = R_4$, $X_{C_3} \gg R_3$), which increases the gain of the amplifier. When the cut-off frequency is less than

the input signal ($f \gg f_c$), impedance of R_4C_3 is dominated by the capacitor C_1 ($R_4 \parallel C_3 = X_{c3}$, $X_{c3} \ll R_3$), reducing the gain of the amplifier to unity.

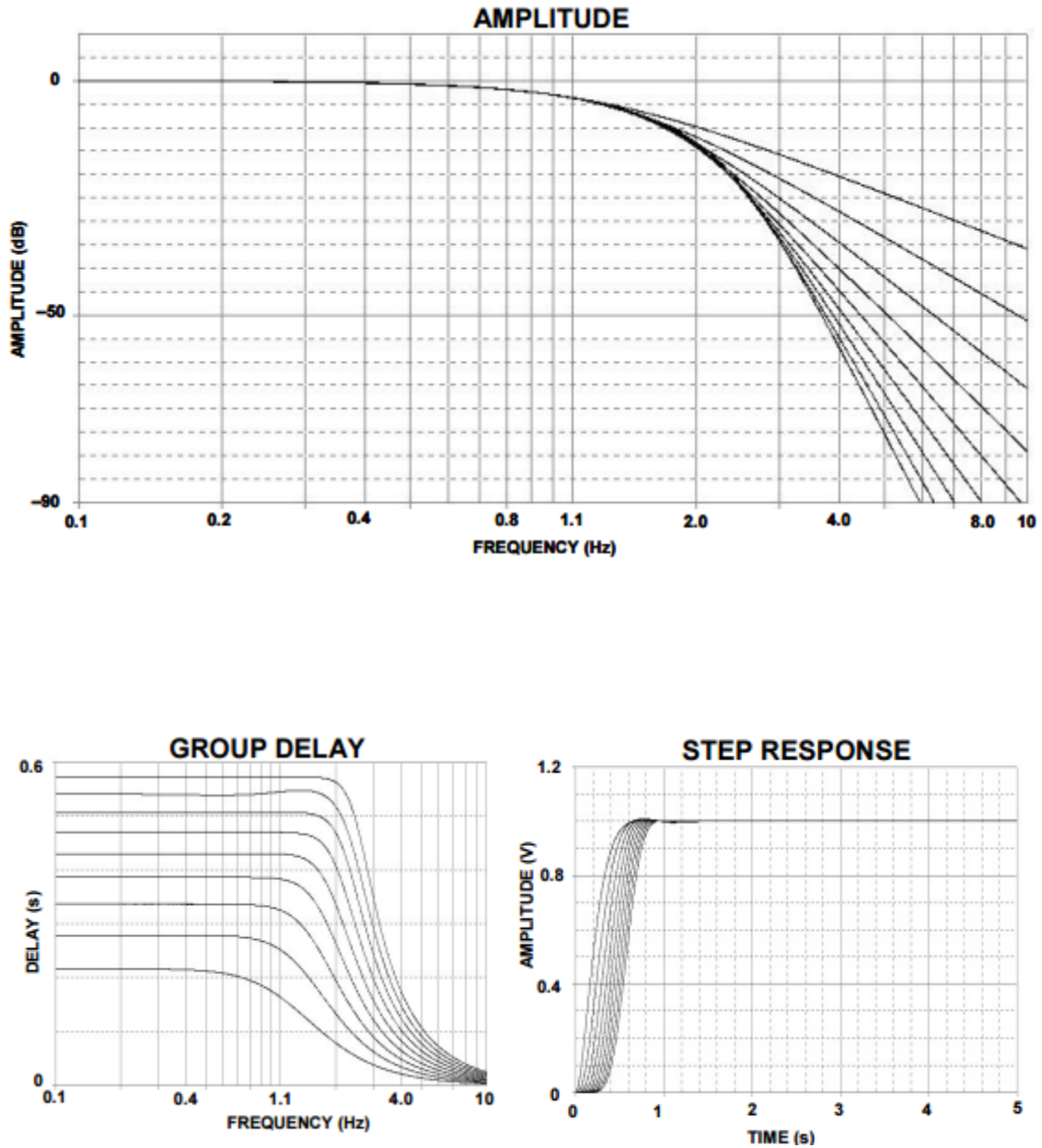


Figure 3.5 – Frequency response, group delay and step response of Bessel filter ^[22]

3.3. Instrumentation Amplifier

Instrumentation amplifier consists of a differential amplifier with the inputs fed through two buffer amplifiers. Instrumentation amplifiers eliminate the use of input impedance matching and provide low DC offset, low noise, low drift, high open loop gain, high CMRR, high input impedances. A schematic representation of an instrumentation amplifier is shown in the figure below.

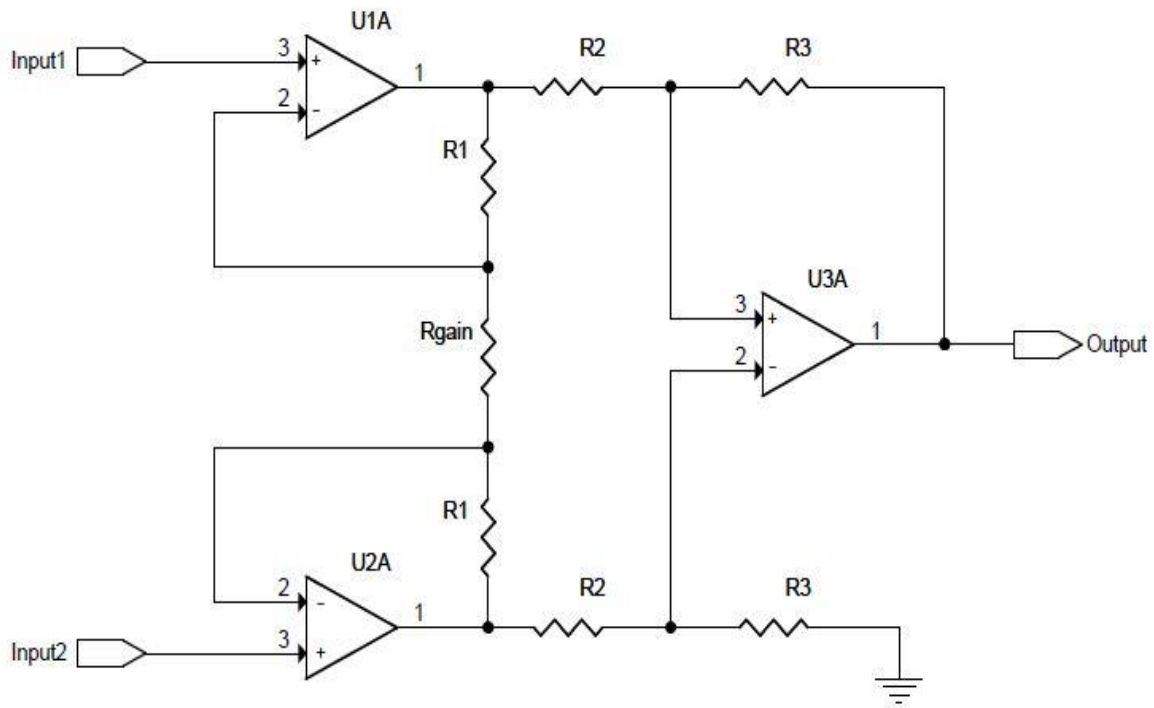


Figure 3.6 - Instrumentation Amplifier

The op-amp U_3 is nothing but a differential amplifier with a gain of R_3/R_2 and differential input resistance $2 \cdot R_2$. Op-amps U_1 and U_2 are just buffer amplifiers where it becomes a unity gain buffer amplifier when R_{gain} is infinity. In this case the overall gain becomes $1 + (R_3/R_2)$. Therefore, R_{gain} is mainly used to enhance the buffers resistant to

common mode signals and as a result it increases the overall gain and the common mode rejection ratio (CMRR) of the circuit.

$$\text{Overall Gain} = \frac{V_{out}}{V_2 - V_1} = \left(1 + \frac{2R_1}{R_{gain}}\right) \frac{R_3}{R_2}$$

4. MEMS ACCELEROMETER

4.1. Introduction

An accelerometer is an electromechanical device which can be used to measure the acceleration of a body relative to free-fall; this can be caused due to static or dynamic forces. Such accelerations are measured in terms of g-force (where $g = 9.81 \text{ m/s}^2$) therefore, at rest the accelerometer indicates 1g upwards. It can also measure tilt, vibration and shock of a body. Due to its low cost and efficiency, accelerometers are widely used in industrial applications, mobile phones, tablets, inertial navigation systems, vibration detectors, drones, digital cameras, joysticks and so on.

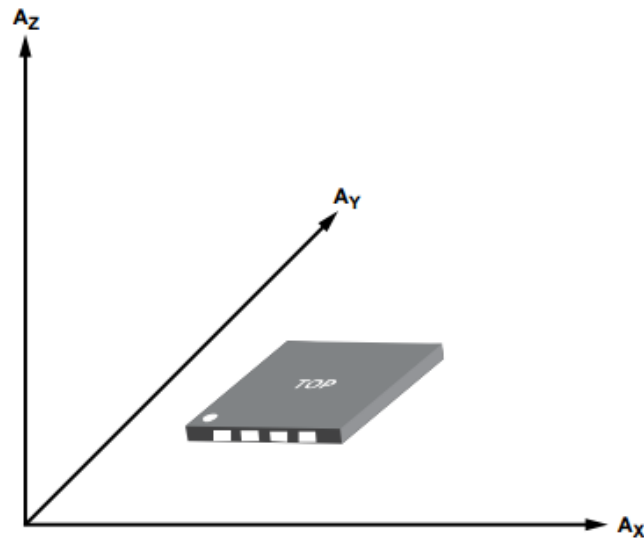


Figure 4.1 – Axes of acceleration sensitivity ^[23]

MEMS or Micro Electro Mechanical Systems are nothing but small electro-mechanical devices consisting of structures ranging in size between 1-100 μm . MEMS structures includes cantilevers, holes, cavity, etc. As a whole, a MEMS device measures from 20 μm to 1 mm.

4.2. Technical Specification

Device	ADXL335
Measurement Range	$\pm 3.6g$
Sensitivity	270-330mV/g
Output Voltage	1.2-1.8V
Frequency Bandwidth	1600Hz
Power Supply	1.8 – 3.6V
Operating Temperature	-40 - +85 °C
Package	LFCSP_LQ (4 x 4 x 1.45mm)

Table 4.1 – Technical specifications of Accelerometer ^[23]

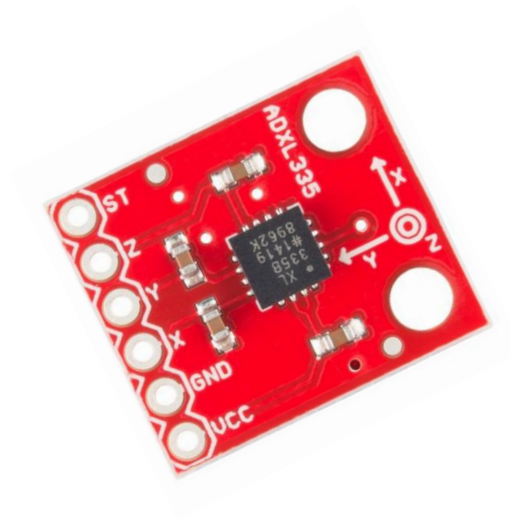


Figure 4.2 – ADXL335 Triple Axis Accelerometer

5. BLUETOOTH – WIRELESS PROTOCOL

5.1. Introduction

Bluetooth technology was originally developed by Ericsson in 1994 to enhance their smartphones to sync and communicate with a PC without using a conventional RS-232 cable. Bluetooth is one among many wireless technologies which is capable of transmitting a secure and lossless data over short distances. Other features of Bluetooth include ubiquitousness, low cost and low power. Currently, Bluetooth is managed and controlled by Bluetooth Special Interest Group (SIG) which means, SIG monitors the specifications, development and trademarks of Bluetooth and also a manufacturer must meet SIG standards to market a product as Bluetooth device. Depending upon the range of operation, Bluetooth devices are classified into Class1, Class2 and Class 3 devices. Class 1 has a range of about 100meters, Class 2 has about 10meters and Class 3 has about 1meter range ^[24].

The IEEE standard for Bluetooth protocol is IEEE 802.15.1 and it works based on the master-slave principle. The Bluetooth protocol stack consists of the following layers: transport layer, middleware layer and application layer. The transport layer consists of radio, baseband and link layers. The middleware acts as a software tool to establish better communication layers ^[25]. Bluetooth protocol uses Phase Shift Keying (PSK), Frequency Shift Keying (FSK) and Spread Spectrum (SS) as modulation schemes.

Bluetooth v2.0+EDR extension was specially developed to improve the data rate of the communication. EDR extensions use $\pi/4$ -Phase Differential Quaternary Phase-Shift Keying ($\pi/4$ -DQPSK) and 8-Phase Differential Phase-Shift Keying (8DPSK) modulation but have no FEC ^[25].

5.2. Technical Specifications

Data Rate	1 - 3Mbps
Range	10 - 100m
Power Consumption	< 1W
Network Topology	Scatternet
Spectrum	2.4 - 2.485GHz
Spectrum Acceptance	Worldwide
Robustness	Adaptive fast frequency hopping
Security	56/128-bit AES Encryption
Slaves	1 - 7

Table 5.1 – Technical specifications of Bluetooth Technology ^[26]



Figure 5.1 – Bluetooth HC-05 Module

5.3. Advantages of Bluetooth over other Communication Protocols

Bluetooth vs. Wi-Fi

- Wi-Fi is a wireless replacement for high speed cables which carry huge data; whereas, Bluetooth can only handle $1/10^{\text{th}}$ of the same data. This means Wi-Fi cost more and consumes more power when compared to Bluetooth modules.

Bluetooth vs. Zigbee

- Zigbee is capable of handling lossless data up-to 250kbps. Module loses data beyond 250kbps, to improve the transmission efficiency. For our application, the data sampling rate is high and any loss of data leads to incorrect results. Bluetooth can handle up-to 1Mbps without losing data and it is present in all mobile phones, PDAs and computers which make the interface more user-friendly.

Bluetooth vs. GSM

- GSM can communicate over a huge area, but transmitting sensitive data involves high risk. GSM communication has less security than when compared to 128-bit AES encrypted Bluetooth communication. Also, GSM modules need excellent towers for lossless transmission. Finally, the power consumption is higher in GSM when compared to Bluetooth.

Bluetooth vs. Infrared

- Infrared communication is way cheaper than Bluetooth. But infrared communication needs a clear sight of view between the transmitter and the receiver modules, which is not necessary in the case of Bluetooth. Bluetooth can handle data transmission up to 100m outdoor and up to 30m indoor.

6. SYSTEM DESIGN

The prototype's operation and design is best understood in this chapter. The first subsection gives you an overall insight on how the data is collected and processed. The other two sub-sections detail the hardware and software implementation in order to make the prototype work.

6.1. Introduction

The prototype implementation of this thesis involves both hardware and software. The hardware section consists of smart band and a transmitter module. The arm band has a 3-axis MEMS accelerometer and three sEMG (surface EMG) electrodes which help to pick-up the bio-potential signals. The transmitter module consists of analog front end amplifiers, ARM processor, an HC-05 Bluetooth module and the power supply circuit. The power supply to the transmitter is provided by two Polymer Lithium Ion batteries. The analog front end amplifiers not only amplify the bio-potential signals but also remove noise. The amplified signal is then fed to the ARM microcontroller which converts the analog data into digital data. On selective intervals, i.e. when the microcontroller senses a sudden spike above a set threshold, the microcontroller starts recording the data for the next 500ms. This data is then sent to the receiver by a Bluetooth module interfaced to the microcontroller.

The receiver section, normally a PC, has another Bluetooth module paired with the transmitter. Other than the Bluetooth receiver module, it only consists of software. The data transmitted is received by the receiver Bluetooth module and then logged using MATLAB

toolbox for feature extraction and to identify the gesture. The offline processing in the receiver is detailed in the software section. Figure 6.1 shows the overall architecture of the system which includes both hardware and software

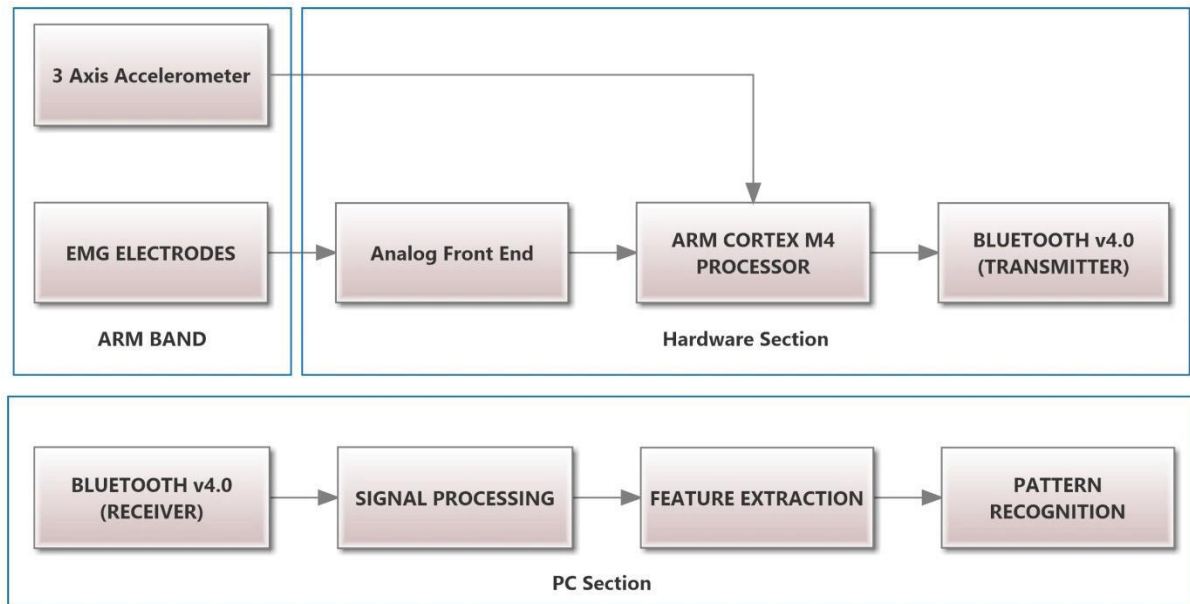


Figure 6.1 – System Design

6.2. Hardware Design

Collecting bio-potential signal and amplifying is fundamental in this thesis. It is the hardware section that picks up the signal, amplifies, converts analog to digital and finally transmits the digital data to a nearby receiver. To do this, the hardware consists of sensors, analog front end amplifiers, ARM microcontroller and a Bluetooth module. Individual blocks of the hardware section are discussed below in detail.

6.2.1. Sensors

A basic passive metal electrode is used to pick up the EMG signals, shown below (Figure 6.2). These metal electrodes are cheaper and do not need any conductive gels which may cause skin allergy or incorrect readings when they dry out. Proper placement of sensors on the forearm is necessary to record noise free data. Two electrodes must be placed on the muscles critically responsible for the flexion/extension of fingers and wrist. To be more precise, electrodes must be placed on the Flexor Digitorum Superficialis muscles to recognize wrist flexion or on Extensor Digitorum muscles to recognize wrist extension [27]. Also note that the electrodes should be placed longitudinal to the muscles and between two motor units and away from the tendons. The other reference sensor can be placed anywhere except the muscles responsible for flexion of fingers or wrist.

A triple axis accelerometer ADXL335 is used to detect the orientation of the wrist. Here, the accelerometer is placed on the posterior side of the forearm. For better results, the accelerometer can be placed on the posterior side of the hand.

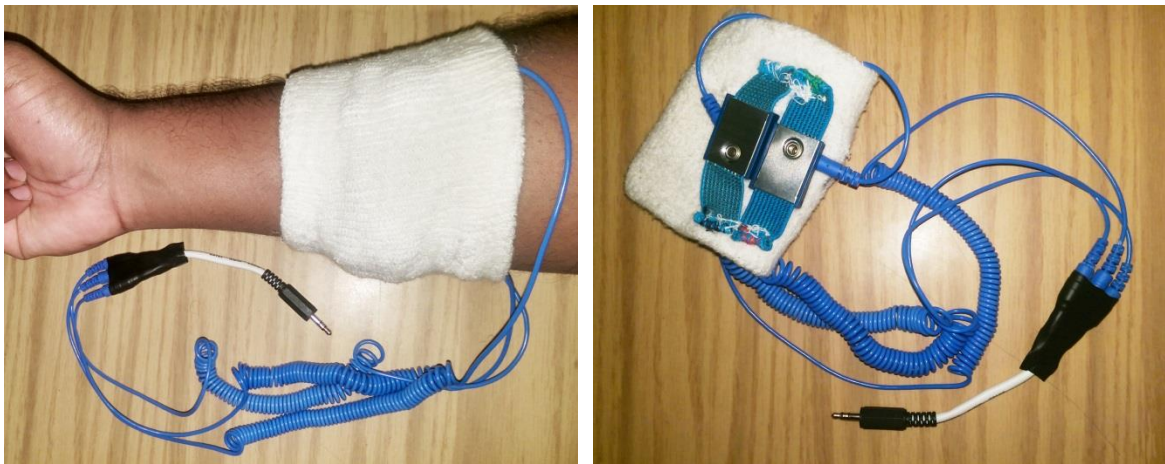


Figure 6.2 – Smart Band

6.2.2. Analog Front End

Bio-potential signals are normally weak and possess huge noises. Significant EMG ranges from a few Hz to 500Hz. Therefore we need to eliminate the noise signals (below 1Hz and above 500Hz) and amplify the weak signals. A functional block diagram along with the schematic of the analog front end amplifiers is shown below in the figure 6.3 and figure 6.4.

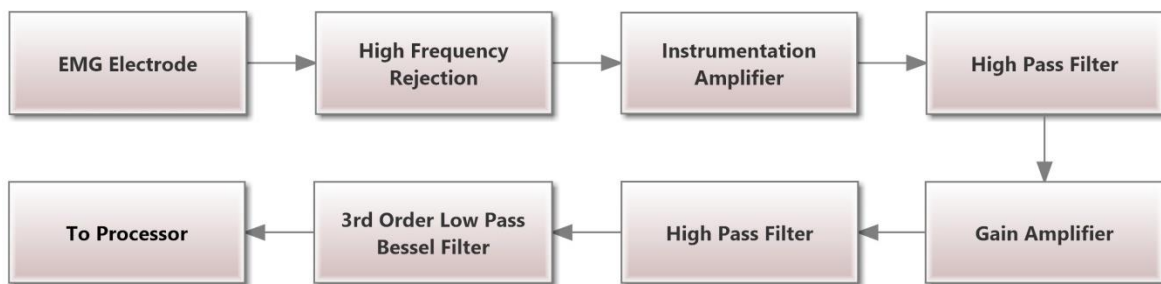


Figure 6.3 – Front End Amplifier Design

The front end amplifier consists of 4 components, namely: High frequency rejection block, instrumentation amplifier block, non-inverting gain amplifier bloc and a Bessel filter block. The instrumentation amplifier and gain amplifier is solely responsible for signal amplification. High pass filters and Besselworth filter are used to filter noises above and below the individual cut-off frequencies. Only the EMG signal requires this attention as it has low potential and more noise. The accelerometer signal does not need any amplification or noise filtering blocks as it is already filtered and amplified within the accelerometer IC. The analog section has a separate analog grounding and reference voltage block to improve the signal conditioning.

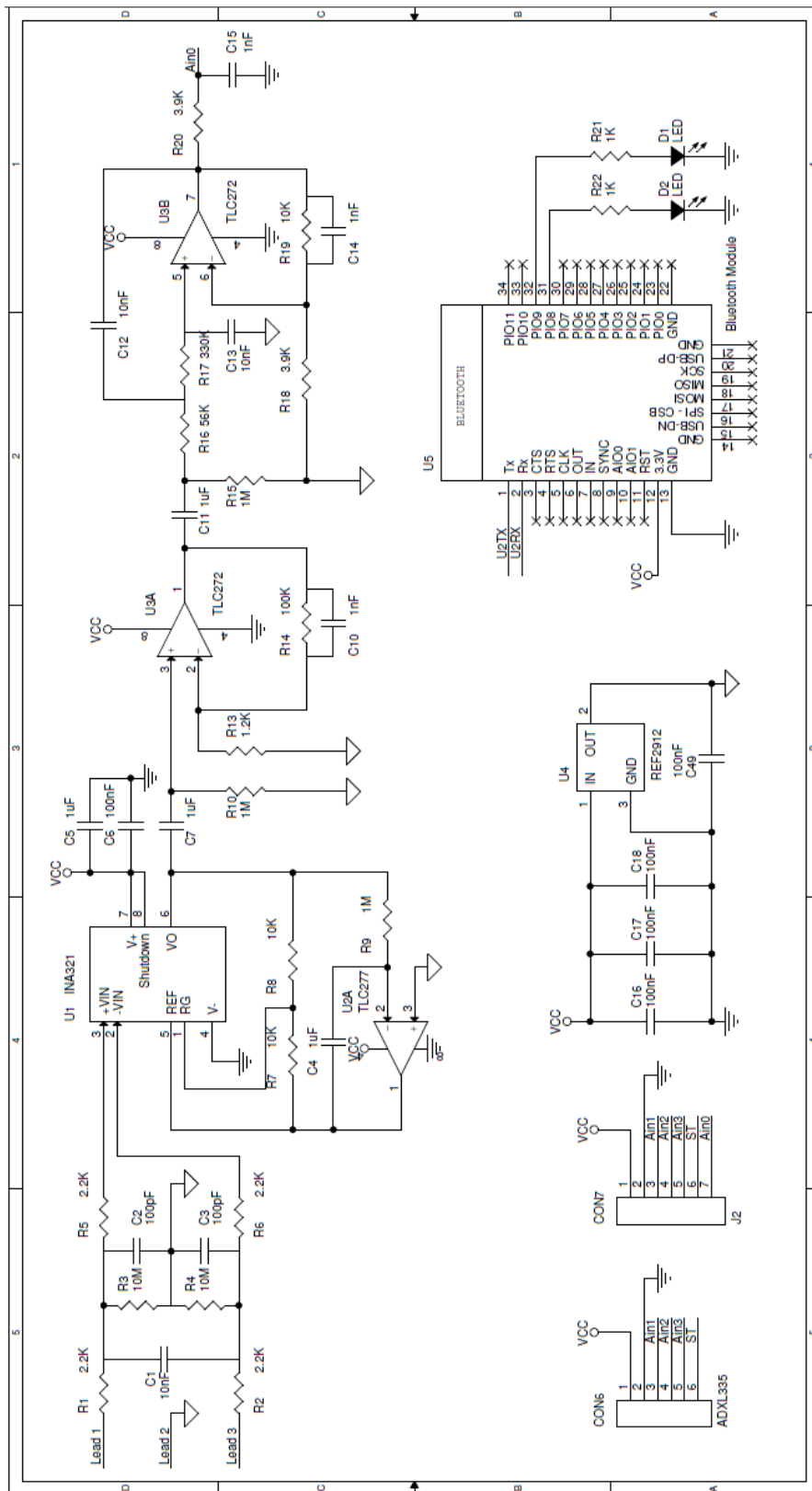


Figure 6.4 – Analog Front End and Bluetooth - Schematic

High Pass Filter: The cut-off frequency of all the first order high pass filters is set to 0.1Hz, i.e. all frequencies below 0.1Hz are filtered as noise. The passive high pass filter not only filters low frequency signals but also blocks DC components present in the signal. Therefore, this is repeated at every stage.

Instrumentation Amplifier: A Single supply INA321 instrumentation amplifier is used to amplify the difference between the two input voltages. The gain of the amplifier is set to 10, which is derived by the formula:

$$\text{Gain of Instrumentation Amplifier, } A = 5 * \left(1 + \frac{R8}{R7}\right)$$

Non-Inverting Amplifier: The amplified signal is further amplified by passing through a non-inverting amplifier with a gain of 80. The gain is given by the formula:

$$\text{Gain of Non - Inverting Amplifier, } A = \left(1 + \frac{R14}{R13}\right)$$

3rd Order Bessel Filter: The Bessel filter is the last stage of front-end amplifier where a low pass filter is planted with a cut-off frequency of 40Hz to filter out frequencies more than 50Hz. The gain is set to 3.5 and given by the formula:

$$\text{Gain of 3rd Order Besselworth Filter, } A = \left(1 + \frac{R19}{R18}\right)$$

Reference Voltage: A virtual ground is implemented using REF2912 to measure the EMG signal with a complete set of positive components. TI's REF2912 virtual ground IC keeps the reference voltage at 1.25V. The circuit diagram is shown in figure 6.4.

6.2.3. Microcontroller

The CPU block is nothing but a microcontroller itself which does the analog to digital conversion and transmission part. TM123GH6PM is a 32-bit microcontroller embedded in the smart band. It has an ARM Cortex M4F processor core designed for small embedded applications. It is an ultra-low power device that supports up to 80MHz of clock speed. It has 256 KB of flash memory and 32KB of SRAM memory to store and run the program ^[28]. A schematic of the CPU block is shown below in the figure 6.5.

ADC Module: The microcontroller has a 12-bit precision ADC module with a maximum sampling rate of 1 million samples per second. The ADC module is isolated from the normal working of microcontroller, i.e. ADC samples the data and stores it in the buffer even when the microcontroller is busy performing other tasks. This enables the microcontroller to preserve the signal especially when it is busy transmitting the data to Bluetooth ^[28].

USART Module: The microcontroller has 8 built-in USART (Universal Synchronous Asynchronous Receiver Transmitter) ports with maximum baud rate of 5Mbps. USART falls under the serial communication category and supports full duplex. To communicate with Bluetooth the baud rate is set to 115200 bps ^[28]. The data is framed before transmission so as to make the receiver identify the start and end of a data set.

Timer Module: The microcontroller has six 16/32 bit and six 32/64 bit programmable timers. A timer is necessary to track the transmission time of each data set. The timer should start when muscle activity is sensed and should stop the transmission at the end of 500ms. At the end of transmission the timer must reset to its initial value. For this, the microcontroller is programmed to use one 16 bit timer ^[28].

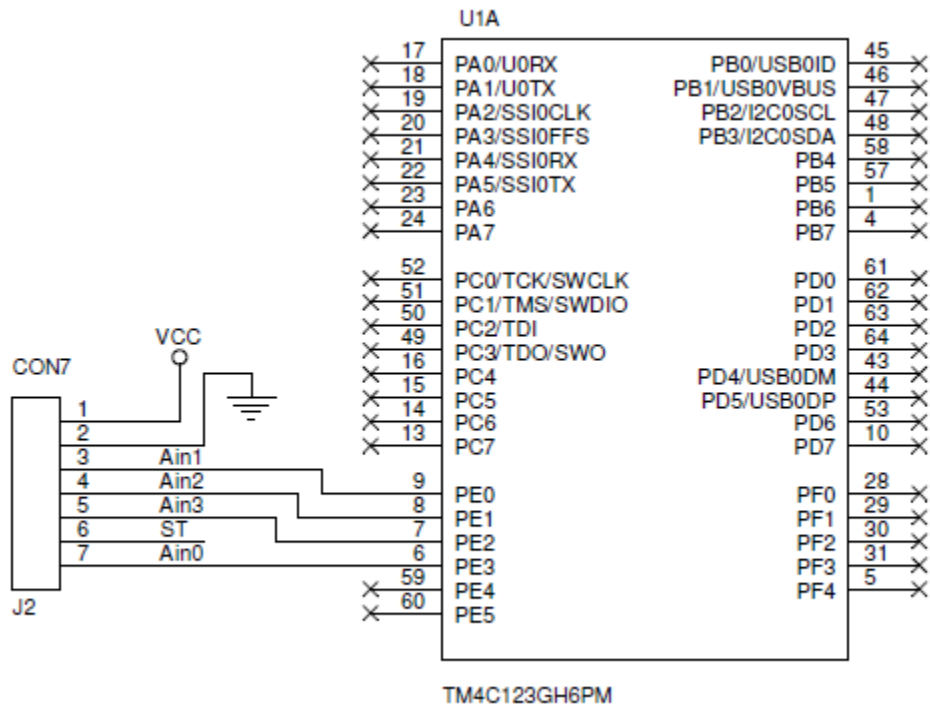
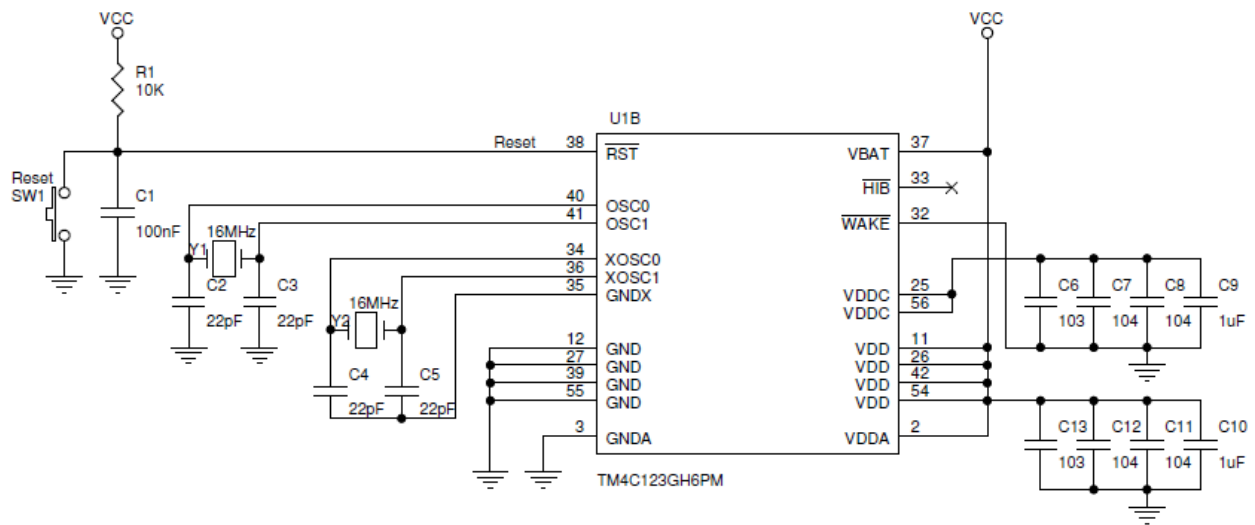


Figure 6.5 – Microcontroller (CPU) - Schematic

6.2.4. Wireless Transmission

Bluetooth communication is held by a device HC-05 which is interfaced with the microcontroller. HC-05 is a fully qualified Bluetooth v2.0+EDR (Enhanced Data Rate) having up to 3Mbps of data rate. The module has a CSR Bluecore chip which is responsible for the communication. Initially, a communication channel must be established to create a transparent port, i.e. to transmit and receive data transparently without encoding or decoding the data. The Bluetooth is programmed to communicate at a speed of 115200 bps. The framed data is received by a UART port present in the Bluetooth module.

6.3. Software Design

The software section involves two operations: making the microcontroller to transmit the data and to decode the raw EMG data for identifying the gestures. To do this, the first operation is done within the microcontroller and the later using a PC. Both the sections are briefly discussed below.

6.3.1. Transmitter Section

The software of the transmitter does the work of converting analog data into digital and making the Bluetooth to transmit data to the receiver section. An ARM Cortex microcontroller is used to perform this task; therefore, the software is written using Embedded C language.

At first, the microcontroller is programmed to initiate the UART, ADC and timer modules. UART module is responsible to establish a communication between microcontroller and HC-05 Bluetooth module. A 16-bit timer module is initiated to keep track of transmission period. The ADC module is set to use 4 ADC channels (one for EMG and three for accelerometer) with 12-bit precision (i.e. for a full scale 0-3.3V measurement, output ranges from 0-4096). Therefore, the microcontroller is interfaced with the front-end analog circuit which measures the EMG and accelerometer signal voltages and converts it to a digital format using an ADC module inbuilt within the microcontroller. This conversion is done at a sampling rate of 1600 Hz (i.e. 1600 samples per second). The ADC module dumps the digital data into a large buffer where the data is temporarily stored and fires an interrupt to let the processor know that the conversion is done. The ADC flushes the data from its buffer once the processor accesses it. The microcontroller continuously monitors the EMG analog channel for a voltage spike above the set threshold. When a spike occurs, the processor is programmed to start a 16-bit timer and send the data to Bluetooth for the next 500ms. When the timer reaches 500ms, it stops the transmission and resets the timer. Before the transmission, one full set (i.e. one EMG data along with accelerometer data at one instance) of data is encoded to fit in a frame. Frame of the data is fixed and has a start and stop bit. Framing of data helps the receiver to identify the start and end of a data set. This frame is then sent to the Bluetooth module over a UART port (serial communication) which is programmed to handle 115200 bps. The serial port has inbuilt flow control and packet acknowledgement features which helps in transmitting data with no loss. The HC-05 module receives the data using same the serial port embedded in it and sends the data to the receiver once the communication channel is established.

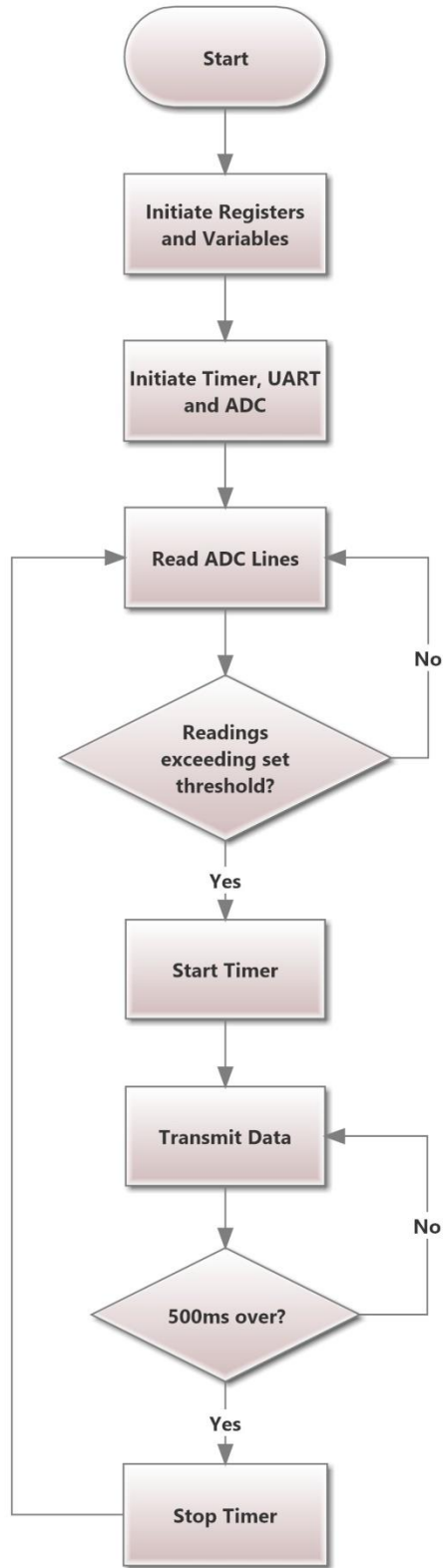


Figure X.X – Transmitter Software Flow

6.3.2. Receiver Section

The receiver's software section plays the major role in this thesis which involves shaping, noise filtration, feature extraction and pattern recognition. The entire process is done offline to keenly evaluate and analyze each step. This section is done using MATLAB software as a simulation tool. The receiver Bluetooth module receives the data and sends it to the PC via serial port. This data is captured by the MATLAB using a serial port access tool. The baud rate of this communication is again set to 115200 bps, so as to maintain good transfer flow between the transmitter and the receiver. The simulation software is programmed to capture the data and log them for future use. At the time of pattern recognition, this data is accessed. Remember that each data set or each pattern is 500ms long. A block diagram representing the receiver's software section is shown in the figure X.X and each block is detailed below. The second stage of the simulation software involves shaping the raw EMG signal. For this, the EMG signal is passed through a full-length rectification block where it converts the negative components into positive components. From there the signal is sent to FIR filter for noise filtering and reducing the frequency of the signal. Feature extraction is done for both EMG and accelerometer signals.

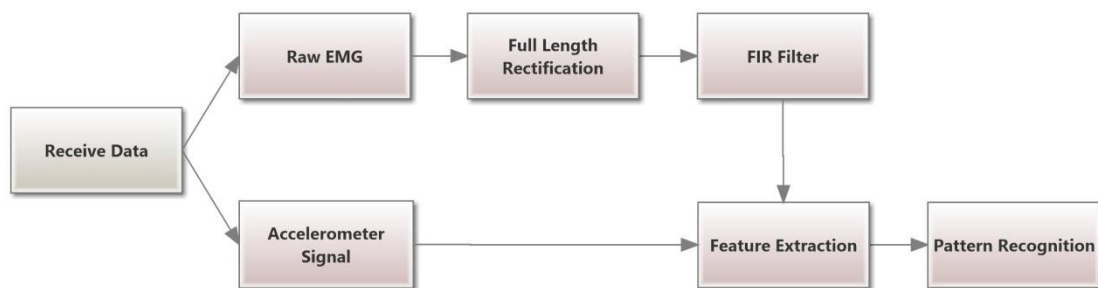


Figure X.X – Receiver Software Flow

Raw accelerometer data has much less noise and therefore it can be directly used for feature extraction. Finally, multi-class SVM technique is employed to train and classify the patterns based on features extracted.

Full Wave Rectification: Raw EMG data has both positive and negative components present in it. The presence of negative components suppresses the features when we take mean. This may lead to loss of information in sensitive cases. To overcome this, the raw EMG signal can be half-length or full-length rectified. Half-length rectifies the negative components which may again lead to loss of information. Whereas, full-length rectification overcomes this problem as it converts the negative components to positive components of the signal.

FIR Filter: FIR filters are finite impulse response digital filters and it can handle a finite series of data with more stability and linearity when compared to an IIR (Infinite Impulse Response) filter ^[29]. FIR filter with a Hamming window of order size 48 is implemented in the filtering section. The sampling rate of this filter is 1600 Hz and the cut-off frequency is set to 250Hz. As a result of windowing, a 30ms delay is introduced. A mathematical representation of FIR filter is given by,

$$y(n) = \sum_{k=0}^N h(k) x(n - k)$$

where, $x(n)$ represents the filter input,

$h(k)$ represents the filter coefficients,

$y(n)$ represents the filter output,

n is the number of filter coefficients (order)

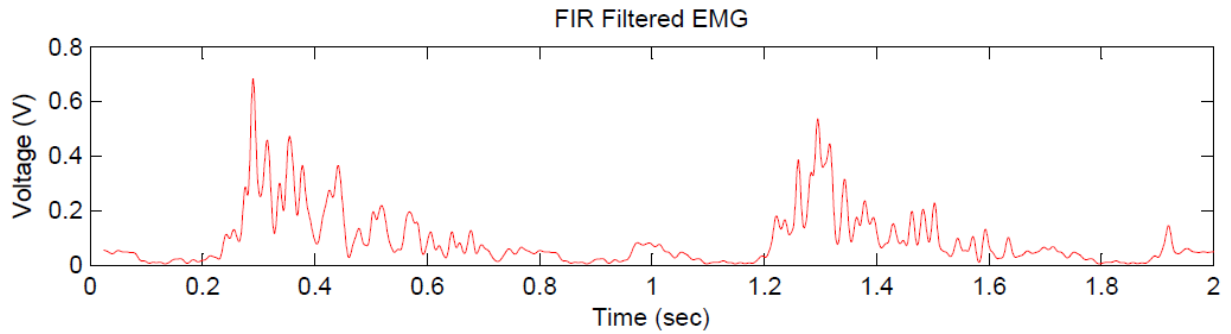
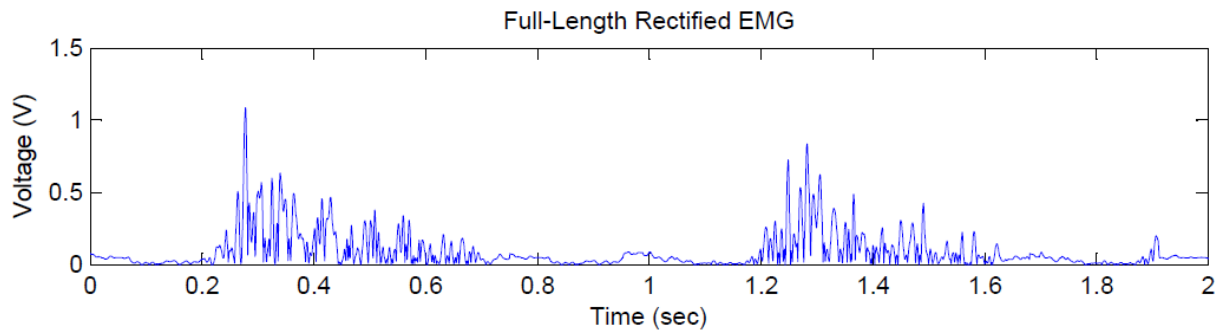
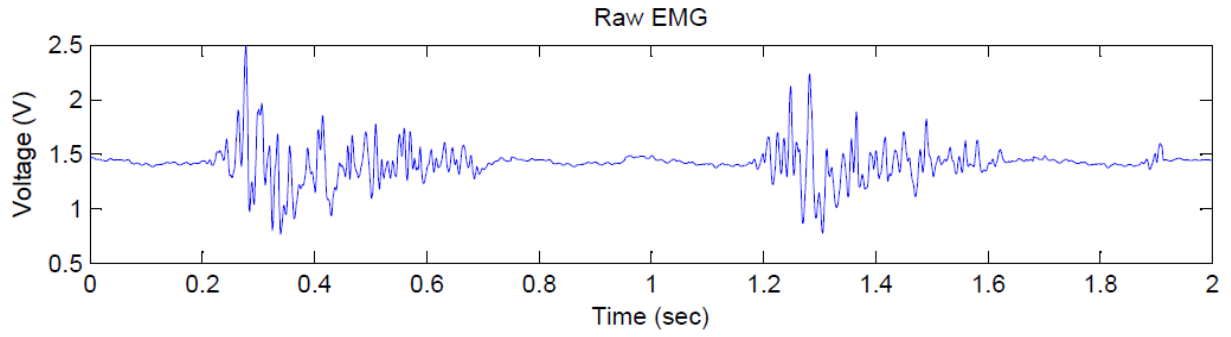


Figure X.X – Raw EMG signal (Top), Full-length Rectified EMG Signal (Middle) and FIR filtered EMG signal (Bottom)

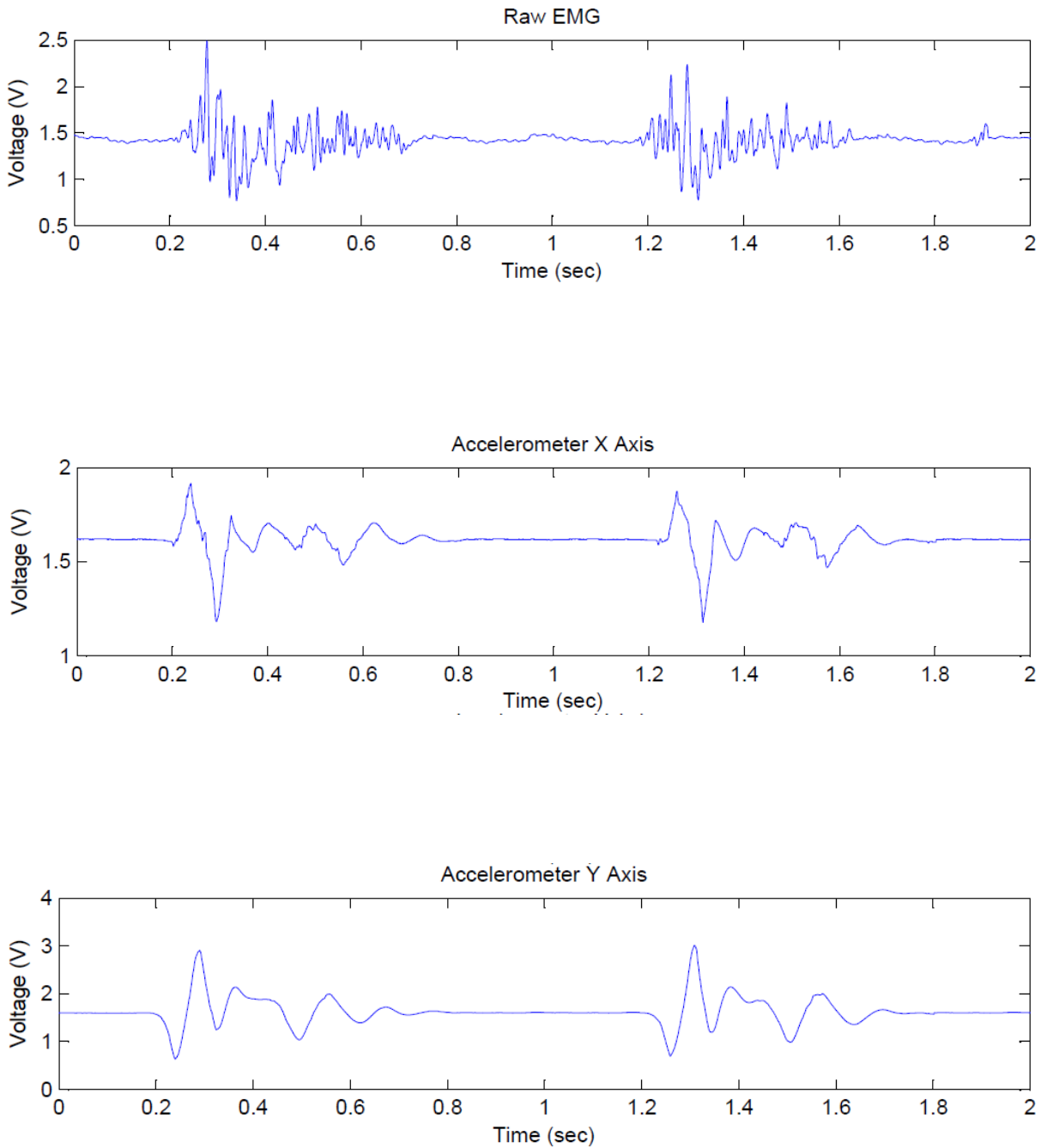


Figure X.X – Raw EMG signal (Top), Accelerometer Reading for X-Axis (Middle) and Accelerometer Reading for Y-Axis (Bottom) during Wrist Pronation

Feature Extraction: Raw EMG signals possess more noise but weighted information remains amalgam in it. Predicting the results based on raw EMG degrades the efficiency of the system to a great extent. For this, certain features carrying the right information are present in time, frequency and time-frequency domains ^[13]. Therefore, considering time domain, five important features such as mean, variance, waveform length, root mean square and threshold crossing are extracted ^[30]. The mathematical representations of these features are as follows:

- $Mean = \frac{1}{N} \sum_{n=1}^N x_n$
- $Variance, VAR = \frac{1}{N-1} \sum_{n=1}^N x_n^2$
- $Waveform\ Length, WL = \sum_{n=1}^N x_{n+1} - x_n$
- $Root\ Mean\ Square, RMS = \sqrt{\frac{1}{N-1} \sum_{n=1}^N x_n^2}$
- $Threshold\ Crossing = \sum_{n=1}^N f(x_n - x_{n+1}) \quad f(x) = \begin{cases} 1, & \text{for } x > \text{threshold} \\ 0, & \text{else} \end{cases}$

Unlike EMG, raw accelerometer readings contain much less noise since the chip does all the necessary processing and filtering. Thus filtered EMG signals along with raw accelerometer readings are passed for feature extraction. The extracted features are then logged to train the system or to recognize the pattern.

Pattern Recognition: SVM is one of the most successful classifiers known in the field of pattern recognition. Multi-class SVM or multiple layers of binary SVM should be adopted since there are five input features and four output classes. There are two types of multi-class SVMs: one-against-all and one-against-one.

The one-against-all approach trains the system to differentiate a class sample from all other class samples by building one class per SVM; whereas, one-against-one builds two classes per SVM (i.e. for n classes, $n(n-1)/2$ SVMs are built) ^[31].

The one-against-one approach results are more promising when a large number of classes are present; on the other hand one-against-all is more practical and accurate for digit classes ^[31]. SVM requires a set of training and test set data for training and testing the system. The training set is fed along with the results and based on these training sets the test data set is predicted for patterns.

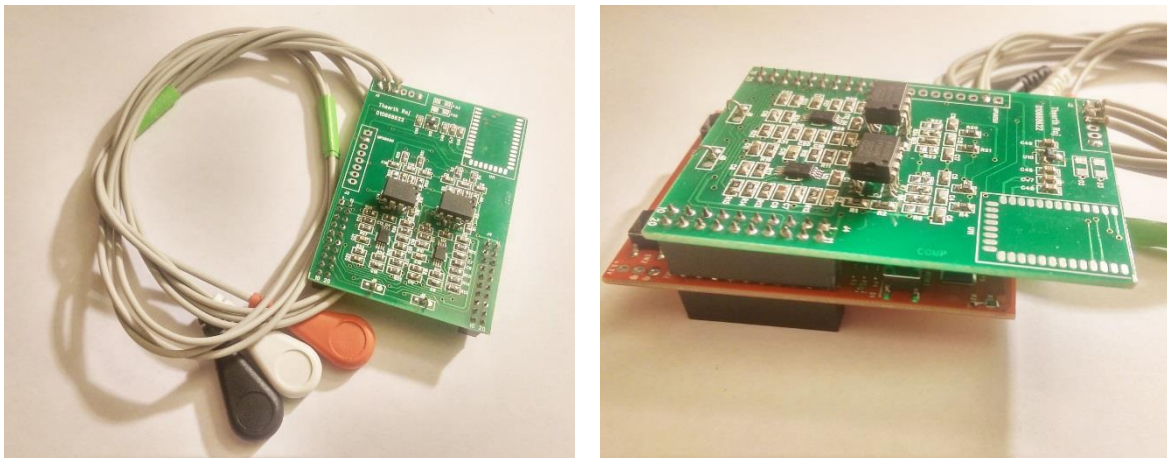


Figure X.X – Transmitter Hardware

7. TEST AND RESULTS

7.1. Testing Procedure

To test and validate the system, large sets of raw EMG and accelerometer readings representing different hand patterns are collected using the hardware. This data is then transmitted to the receiver and processed offline for feature extraction. The feature sets are then randomly split into training set and test set in the ratio of 10:1. Say for example, for each class 110 features are extracted out of which 100 belong to training set and 10 belong to test set.

On the first iteration, only the EMG data sets are used for pattern recognition; during the second iteration, only accelerometer data was taken into account; on the third iteration both EMG and accelerometer data sets are used to recognize pattern. Finally, comparison of all three iteration results, presents us the possibility of recognizing more patterns and the accuracy levels with and without one another.

7.2. Results on Pattern Recognition

Ten classes representing five different hand patterns with two different orientations were accounted. Each class consisted of 25 training sets and 5 test sets; results were computed with and without accelerometer data. Results with only EMG data predicted only four hand gestures; results with only accelerometer predicted only six patterns. Whereas, results computed with both the features was able to identify all 10 patterns with more accuracy.

8. CONCLUSION AND FUTURE DEVELOPMENTS

Hand pattern recognition techniques predict more patterns with higher accuracy levels when both hand movements and hand gestures are taken into account. To highlight this, EMG and accelerometer readings were first logged while exhibiting a hand pattern. This data is sampled and transmitted by a microcontroller and a Bluetooth module. Another Bluetooth receiver paired with the transmitter receives the signal and provides it to the MATLAB toolbox for filtering and feature extraction. These features are processed through multi-class SVM classifier by three different possibilities: only EMG features, only accelerometer based features and finally both features combined. The results proved that more patterns can be recognized with increased accuracy when both the feature sets are treated at the same time. Advancement and future developments of this thesis may include integrating a third set of feature sets representing the speed of hand movements.

REFERENCES

- [1] Mills K R, "The Basics of Electromyography," in *Journal of Neurology Neurosurgery Psychiatry*, 76th ed. London, UK: JNN, 2005, 76, ii32-ii35.
- [2] Paul E Barkhaus MD. EMG Evaluation of the Motor Unit - Electrophysiologic Biopsy [Online]. Available: <http://emedicine.medscape.com/article/1846028-overview>
- [3] Saksit Siriprayoonsak. Real-Time Measurement of Prehensile EMG Signals (Chapter 2) [Online]. Available: <http://medusa.sdsu.edu/Robotics/Neuromuscular/Theses/Saksit/Saksit.htm>
- [4] Neuman M R, "Biopotential Electrodes," in *The Biomedical Engineering Handbook: 2nd ed.* Florida: CRC Press LLC, 2000, sec. 48.2.
- [5] Dr. Schotty Day, Important Factors in Surface EMG Measurement [Online]. Available: http://andrewsterian.com/214/EMG_measurement_and_recording.pdf
- [6] C. J. De Luca, 1997, "The Use of Surface Electromyography in Biomechanics", *Journal of Applied Biomechanics*, 13, Boston: pp. 135-163.
- [7] Weir J P, Wagner L L, Housh T J (1992). "Linearity and reliability of the IEMG v. torque relationship for the forearm flexors and leg extensors". *American Journal of Physical Medicine and Rehabilitation* 71 (5): pp. 283–287.
- [8] Vrendenbregt J, Rau G, Housh (1973). "Surface eletromyography in relation to force, muscle length and endurance," in *New developments in electromyography and clinical neurophysiology*: pp. 607–622.
- [9] Sushmita Mitra and Tinku Acharya, "Gesture Recognition: A Survey" in *IEEE Transaxtions on System, MAN, and Cybernetics – Part C Applications and Reviews*, vol. 37, no. 3, May 2007. doi: [10.1109/TSMCC.2007.893280].
- [10] Davies A M C, Tom Fearn, "Back to Basics: The Principles of Principal Component Analysis," in *Tony Davis Column*, London, UK: JNN, 2005, 76, pp. 2.
- [11] Wolfram. Wavelet Analysis [Online]. Available: <https://reference.wolfram.com/language/guide/Wavelets.html>
- [12] Chowdhury R H, Reaz M B I, Ali M A B M, Bakar A A A, Chellappan K, Chang T G, "Surface Electromyography Signal Processing and Classification Techniques" in *Sensors* 2013, 13, issn: 12431-12466, doi:10.3390/s130912431
- [13] Anil K Jain, Jianchang Mao, Mohiuddin K M, "Artificial Neural Netwroks," [Online]. Available: <http://csc.lsu.edu/~jianhua/nn.pdf>
- [14] Christopher M BishopPattern, "Recognition and Machine Learning," [Online]. Available: <http://web.mit.edu/zoya/www/SVM.pdf>

- [15] Jiahui Wu, Gang Pan, Daqing Zhang, Guande Qi, Shijian Li, “Gesture Recognition with a 3-D Accelerometer,” in Ubiquitous Intelligence and Computing, 2009, doi: [10.1007/978-3-642-02830-4_4], pp. 25-38.
- [16] Kun Yi, Zhe Yang, “Accelerometer Based Hand Action Recognition” [Online]. Available: https://courses.cit.cornell.edu/ee476/FinalProjects/s2010/ky237_zy49/ky237_zy49/index.html
- [17] Zabulis X, Baltzakis H, Argyros A, “Vision-based Hand Gesture Recognition for Human-Computer Interaction” [Online]. Available: http://www.ics.forth.gr/indigo/pdf/chapter_gestures_submitted.pdf, pp. 1-32
- [18] Meng-Hui Wang, “Hand Recognition Using Thermal Image and Extension Neural Network,” Mathematical Problems in Engineering, vol. 2012, Article ID 905495, 15 pages, 2012. doi:10.1155/2012/905495
- [19] Constantinos S Pattichis, Christos N. Schizas, Lefkos T Middleton, “Neural Network Models in EMG Diagnosis” in IEEE Transactions on Biomedical Engineering. Vol. 42, NO 5. MAY 1995, doi: [10.1.1.461.9863], pp. 2
- [20] Electronics Tutorials [Online]. Available: http://www.electronicstutorials.ws/opamp/opamp_3.html
- [21] Application Report - Active Low-Pass Filter Design [Online]. Available: <http://www.ti.com/lit/an/sloa049b/sloa049b.pdf>
- [22] Hank Zumbahlen, “Analog Filters,” in Basic Linear Design, 2007 ed. USA: Analog Devices, Inc. ch.8, pp. 8.37
- [23] Datasheet – ADXL335 [Online]. Available: <http://www.analog.com/media/en/technical-documentation/data-sheets/ADXL335.pdf>, pp. 12
- [24] Jan Magne Tjensvold (2007), “Comparison of the IEEE 802.11, 802.15.1, 802.15.4 and 802.15.6 Wireless Standards” [Online]. Available: <https://janmagnet.files.wordpress.com/2008/07/comparison-ieee-802-standards.pdf>
- [25] Greg Hackmann (2006), “802.15.1 (Bluetooth),” in 802.15 Personal Area Networks [Online]. Available: <http://www.cse.wustl.edu/~jain/cse574-06/ftp/wpans.pdf>
- [26] Datasheet – HC-05 [Online]. Available FTP: ftp://imall.iteadstudio.com/Modules/IM120723009/DS_IM120723009.pdf
- [27] Innerbody [Online]. Available: <http://www.innerbody.com/anatomy/muscular/arm-hand>
- [28] Datasheet – TM4c123GH6PM [Online]. Available: <http://www.ti.com/lit/ds/spms376e/spms376e.pdf>
- [29] V. R. Zschorlich, Digital filtering of EMG-signals, Electromyography Clinical Neurophysiology, 29 (1989), pp. 81–86

[30] Angkoon Phinyomark, Chusak Limsakul, Pornchai Phukpattaranont, "A Novel Feature Extraction for Robust EMG Pattern Recognition" in Journal of Computing. Vol 1, issue 1, December 2009, ISSN: 2151-9617

[31] Jonathan Milgram, Mohamed Cheriet, Robert Sabourin, "One Against One" or "One Against All": Which One is Better for Handwriting Recognition with SVMs?. Guy Lorette. Tenth International Workshop on Frontiers in Handwriting Recognition, Oct 2006, La Baule (France), Suvisoft.

APPENDIX

```
clear all;
close all;
clc;
```

```
%Temp
% {
RMS_Final = [];
Var_Final = [];
Threshold_Final = [];
Mean_Final = [];
Wavelength_Final = [];
%Final = [RMS_Final Var_Final Threshold_Final Mean_Final Wavelength_Final]
% }
```

```
%Fetch Data_____
%raw_data = csvread('FingerPopping3.csv',1,0); %-1
%raw_data = csvread('HandTwist5.csv',1,0);
%raw_data = csvread('MiddleFingerFlexion5.csv',1,0);
%raw_data = csvread('RingFingerFlexion5.csv',1,0); %-1
raw_data = csvread('WristCloseTightandLight4.csv',1,0);
%plot(Raw_Data(:,1),Raw_Data(:,2));
%legend('Raw EMG');
%xlabel('Time (sec)');
%ylabel('Voltage (V)');
```

```
%FIR Filter_____
sample_rate = 1600;
order = 40;
voltage_data = raw_data(:,2);
voltage_data = voltage_data-1.4;
voltage_data = abs(voltage_data);
fir_coeff = fir1(order, 50/800);
%fvtool(fir_coeff, 'Fs', sample_rate);
filtered_signal = filter(fir_coeff, 1, voltage_data);
```

```
%Plot_____
figure(1);
subplot(2,1,1) % Raw EMG - First subplot
plot(raw_data(:,1),voltage_data)
title('Raw EMG');
xlabel('Time (sec)');
ylabel('Voltage (V)');
```

```

subplot(2,1,2) % Filtered EMG - Second subplot
%plot(Raw_Data(:,1),filtered_signal,'r')
plot(raw_data(order:end,1), filtered_signal(order:end,:), 'r');
title('Filtered EMG');
xlabel('Time (sec)');
ylabel('Voltage (V)');

% Window
Data
-----
windowed_data=[];
i=1;
for j = 1:size(filtered_signal)/1599;
    for i = i:size(filtered_signal);
        if (filtered_signal(i)>0.2);
            windowed_data = [windowed_data filtered_signal(i:i+498)];
            i=i+498;
            break
        end
    end
end

%Plot Windowed Data
-----
for i = 2:size(windowed_data,2)+1;
    figure(i);
    subplot(2,1,2)
    plot(windowed_data(:,i-1))
    subplot(2,1,1)
    plot(filtered_signal);
end

%Feature Extraction
-----
RMS_Samples = rms(windowed_data,1); %Absolute Value Measurement
VAR_Samples = var(windowed_data,1); %Power Density Measurement
Threshold_Crossing = sum(windowed_data>0.25,1); %Samples Exceeding Threshold
1.6V
Mean_Samples = mean(windowed_data,1); %Mean Value
Wavelength_Samples = sum(abs(diff(windowed_data)));%Cummulative absolute difference
between samples

RMS_Final = [RMS_Final;RMS_Samples']
Var_Final = [Var_Final;VAR_Samples']
Threshold_Final = [Threshold_Final;Threshold_Crossing']

```

```
Mean_Final = [Mean_Final;Mean_Samples']  
Wavelength_Final = [Wavelength_Final;Wavelength_Samples']
```

```
%Plot  
x = [1;2;3;4];
```

```
figure(2);
```

```
subplot(2,2,1);  
scatter(x,Mean_Samples,40,'filled')  
axis([0,5,0,2]);  
title('Mean');
```

```
subplot(2,2,2);  
scatter(x,RMS_Samples,40,'filled')  
axis([0,5,0,2]);  
title('RMS');
```

```
subplot(2,2,3);  
scatter(x,VAR_Samples,40,'filled')  
axis([0,5,0,0.05]);  
title('Variance');
```

```
subplot(2,2,4);  
scatter(x,Wavelength_Samples,40,'filled')  
axis([0,5,0,15]);  
title('Wavelength');
```